Supporting Information:

Long Range Charge Transfer (LRCT) Driven Enhancement of SOC and rISC in Donor-Modified MR-TADF Emitters

Hanqi Wen[1] and Liviu Ungur*[1]

[1]Department of Chemistry, Block S8 Level 3, 3 Science Drive 3, Singapore 117543.

*Email: chmlu@nus.edu.sg

List of Figures

List of Tables

Database Supporting Information

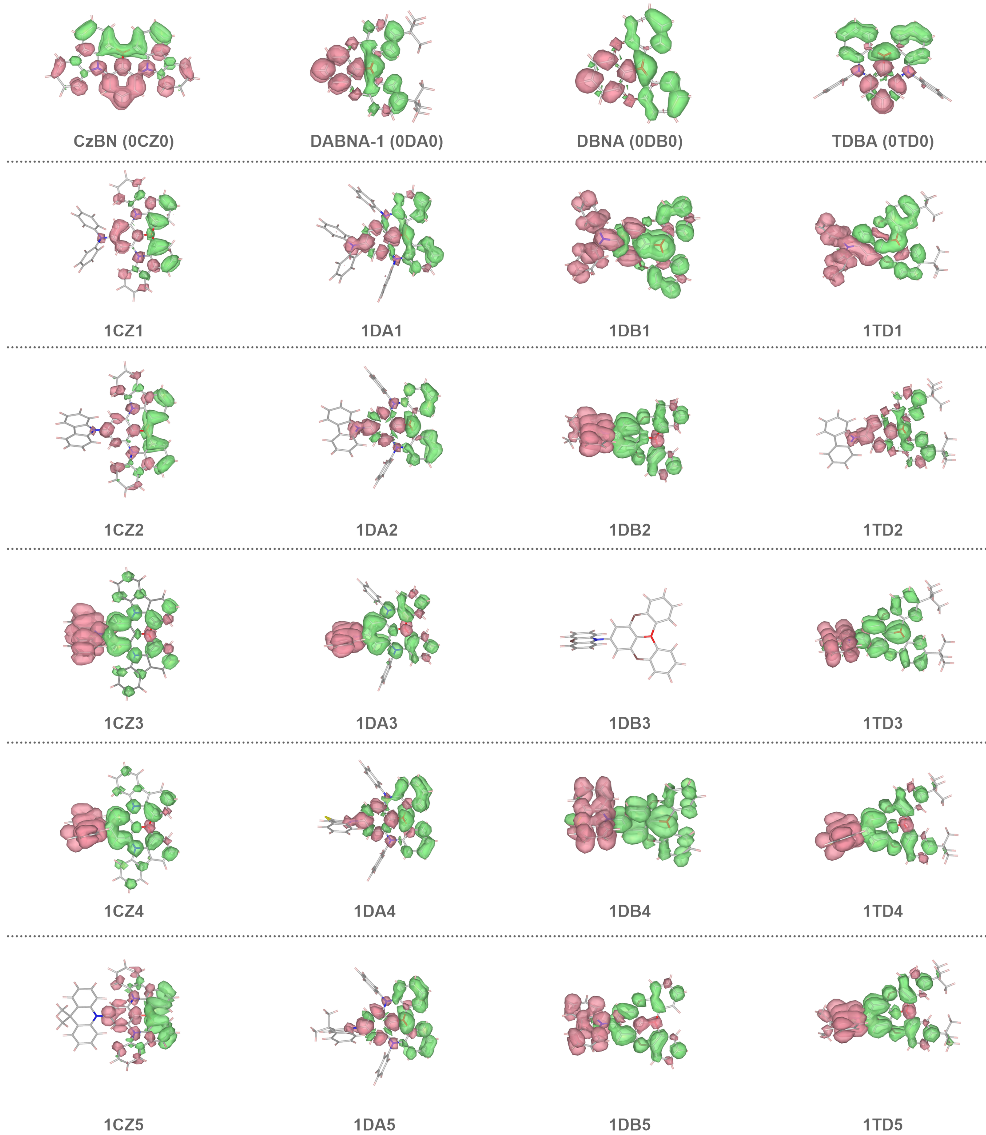

Figure S1: Electron Density Difference between S1 and T1. (isoValue=0.0001, for candidate molecules: isoValue=0.0005) 1DB3 presents no transition under this isovalue due to its high overlap at S_1 and T_1.

Table S1: Energy Gap between S_1 and T_1 (eV) for proposed molecules in the database; Experimental data is shown in bracket. (Calculated using TD-DFT, RMSE = 0.395)

	Core	Donor 1	Donor 2	Donor 3	Donor 4	Donor 5
CZ	0.54 (0.12)	0.49	0.54 (0.18)	0.33 (0.13)	0.51	0.54
DA	0.65 (0.18)	0.59 (0.06)	0.64	0.55	0.67	0.67
DB	0.70 (0.15)	0.57 (0.08)	0.69	0.01	0.17 (0.14)	0.18
TD	0.72	0.56	0.71 (0.06)	0.07 (0.01)	0.25	0.30 (0.06)

Table S2: SOCME (cm^{-1}) between S_1 and T_2

Series	Core	Donor 1	Donor 2	Donor 3	Donor 4	Donor 5
CZ	2.9E-01	2.6E-01	2.8E-01	1.8E-01	3.2E-01	3.7E-01
DA	4.0E-01	4.0E-01	4.8E-01	1.1E+00	4.5E-02	4.4E-01
DB	1.2E-01	5.8E-02	2.2E-01	1.1E+00	8.3E-01	2.4E-03
TD	6.2E-02	1.8E-01	1.4E-01	2.0E-01	8.6E-01	7.3E-03

Marcus rate calculations

Table S3: Marcus rate for $k^{\mathrm{M}}_{\mathrm{rISC}}$ and $k^{\mathrm{M}}_{\mathrm{ISC}}$. Candidate molecules discussed in the main text are shown in bold.

Molecule	SOCME (cm^{-1})	λ_{rISC} (eV)	λ_{ISC} (eV)	$k^{\mathrm{M}}_{\mathrm{ISC}}$ (s^{-1})	$k^{\mathrm{M}}_{\mathrm{rISC}}$ (s^{-1})
0CZ0	3.12E-02	0.110121	0.001644	2.87E-23	1.11E+04
0DA0	3.16E-02	0.184215	0.006580	5.15E-13	5.96E+02
0DB0	2.12E-05	0.202393	0.008687	2.78E-17	1.37E-04
0TD0	4.07E-04	0.199251	0.006216	1.02E-21	5.23E-02
1CZ1	2.97E-02	0.096688	0.002646	2.02E-07	1.88E+04
1CZ2	2.54E-02	0.115664	0.002292	6.21E-17	5.94E+03
1CZ3	**1.66E-01**	**0.299207**	**0.261464**	**2.16E+06**	**3.24E+05**
1CZ4	3.28E-02	0.119459	0.002138	3.59E-20	8.34E+03
1CZ5	2.21E-02	0.116077	0.001897	2.37E-22	4.34E+03
1DA1	2.87E-02	0.689164	0.521446	2.85E+04	8.06E+00
1DA2	2.97E-02	0.199188	0.010209	1.33E-07	3.25E+02
1DA3	**5.40E-02**	**0.174921**	**0.031499**	**8.84E+04**	**6.40E+03**
1DA4	4.55E-03	1.089041	1.002593	1.55E+00	2.22E-02
1DA5	3.18E-02	0.204293	0.007539	2.56E-14	2.72E+02
1DB1	1.54E-01	0.656310	0.454298	2.32E+06	1.36E+02
1DB2	**2.42E-01**	**0.212727**	**0.011780**	**2.04E-05**	**1.31E+04**
1DB3	1.56E-01	0.751925	0.719871	1.24E+04	2.55E+03
1DB4	**5.10E-01**	**0.445341**	**0.217317**	**1.43E+08**	**5.01E+03**
1DB5	**2.33E-01**	**0.214508**	**0.141297**	**2.72E+07**	**7.11E+05**
1TD1	1.20E-01	0.230929	0.028352	6.64E+02	2.83E+03
1TD2	1.80E-03	0.687457	0.488664	2.25E+02	1.50E-02
1TD3	**1.86E-01**	**0.175625**	**0.134131**	**1.31E+07**	**1.57E+06**
1TD4	**5.93E-01**	**0.495948**	**0.219219**	**1.68E+08**	**1.06E+03**
1TD5	**2.29E-01**	**0.314151**	**0.182822**	**2.76E+07**	**5.19E+04**

Details of the rISC rate calculation

The reverse intersystem crossing rate constant, k_{rISC}, was estimated using the coupled singlet–triplet kinetic model reported in ref. [1]. The excited-state populations satisfy

$$\frac{d}{dt}\begin{pmatrix}[S_1]\\ [T_1]\end{pmatrix} = \begin{pmatrix} -\left(k_r^S + k_{nr}^S + k_{\mathrm{ISC}}\right) & k_{\mathrm{rISC}} \\ k_{\mathrm{ISC}} & -\left(k_r^T + k_{nr}^T + k_{\mathrm{rISC}}\right)\end{pmatrix}\begin{pmatrix}[S_1]\\ [T_1]\end{pmatrix} \tag{Eq. S1}$$

The prompt and delayed decay constants correspond to the two eigenvalues of this rate matrix. Following ref. [1], the rate expression was simplified using the assumptions $k_r^S \gg k_{nr}^S, k_r^T, k_{nr}^T$, $k_{\mathrm{rISC}} \gg k_r^T, k_{nr}^T$, and $k_p \gg k_d$, which gives

$$k_p \approx k_r^S + k_{\mathrm{ISC}} + k_{\mathrm{rISC}} \tag{Eq. S2}$$

$$k_p k_d \approx k_r^S k_{\mathrm{rISC}} \tag{Eq. S3}$$

With $k_{ISC} \gg k_{rISC}$, Eq. S2 can be written as:

$$k_p \approx k_r^S + k_{\mathrm{ISC}} \tag{Eq. S4}$$

From Eq. S3 and Eq. S4, rISC rate constant can be described as:

$$k_{\mathrm{rISC}} = \frac{k_{\mathrm{p}} k_{\mathrm{d}}}{k_{\mathrm{p}} - k_{\mathrm{ISC}}} \tag{Eq. S5}$$

Table S4: Calculated rISC Rates and parameters Eq. S5 (RMSE of logk = 0.340).

Molecule	k_{p} (s^{-1})	k_{ISC} (s^{-1})	k_{d} (s^{-1})	k_{rISC} (s^{-1})	$k_{\mathrm{rISC}}^{\mathrm{exp}}$ (s^{-1})	Ref
0CZ0	2.79E+08	1.52E+06	2.23E+04	2.24E+04	1.69E+04	[2]
0DA0	1.90E+08	1.55E+06	1.07E+04	1.08E+04	9.90E+03	[3]
0DB0	1.42E+08	3.38E+05	1.52E+04	1.52E+04	1.60E+04	[4]
1CZ2	2.66E+08	1.13E+05	1.09E+04	1.09E+04	7.60E+03	[5]
1CZ3	4.12E+07	7.99E+04	7.14E+05	7.16E+05	2.00E+06	[6]
1DA1	1.65E+08	2.06E+03	1.80E+04	1.80E+04	6.94E+04	[7]
1DB1	3.98E+08	6.37E+04	1.49E+04	1.49E+04	1.91E+04	[8]
1TD2	2.44E+08	6.46E+04	6.21E+04	6.21E+04	6.99E+04	[9]
1TD3	1.73E+07	3.93E+02	8.00E+05	8.00E+05	2.42E+06	[10]
1TD5	1.41E+07	6.01E-01	7.14E+06	7.14E+06	1.76E+06	[11]

Table S5: ESD-calculated elementary radiative rate k_{r} and ISC rate k_{ISC} (s^{-1}) for proposed molecules in the database.

Series	**Type**	**Core**	**Donor 1**	**Donor 2**	**Donor 3**	**Donor 4**	**Donor 5**
CZ	k_{r}	2.78E+08	2.49E+08	2.66E+08	4.11E+07	2.79E+08	2.84E+08
	k_{ISC}	1.52E+06	4.32E+03	1.13E+05	7.99E+04	6.50E+05	1.38E+06
DA	k_{r}	1.88E+08	1.65E+08	1.86E+08	4.58E+07	1.90E+08	1.98E+08
	k_{ISC}	1.55E+06	2.06E+03	1.68E+03	1.07E+07	2.65E+07	6.16E+05
DB	k_{r}	1.41E+08	3.98E+08	3.48E+09	3.09E+02	1.62E+08	1.13E+07
	k_{ISC}	3.38E+05	6.37E+04	1.03E+05	1.20E+01	2.42E+06	3.78E+01
TD	k_{r}	1.58E+08	4.48E+08	2.44E+08	1.73E+07	1.72E+07	1.41E+07
	k_{ISC}	5.25E+05	1.83E+04	6.46E+04	3.93E+02	1.07E+04	6.01E-01

References

(1) Kaji, H.; Suzuki, H.; Fukushima, T.; Shizu, K.; Suzuki, K.; Kubo, S.; Komino, T.; Oiwa, H.; Suzuki, F.; Wakamiya, A.; Murata, Y.; Adachi, C., Purely organic electroluminescent material realizing 100% conversion from electricity to light, *Nature Communications* **2015**, *6*(1), 8476, DOI: 10.1038/ncomms9476.

(2) Xu, S.; Yang, Q.; Zhang, Y.; Li, H.; Xue, Q.; Xie, G.; Gu, M.; Jin, J.; Huang, L.; Chen, R., Solution-processed multi-resonance organic light-emitting diodes with high efficiency and narrowband emission, *Chinese Chemical Letters* **2021**, *32*(4), 1372–1376, DOI: 10.1016/j.cclet.2020.10.022.

(3) Hatakeyama, T.; Shiren, K.; Nakajima, K.; Nomura, S.; Nakatsuka, S.; Kinoshita, K.; Ni, J.; Ono, Y.; Ikuta, T., Ultrapure Blue Thermally Activated Delayed Fluorescence Molecules: Efficient HOMO–LUMO Separation by the Multiple Resonance Effect, *Advanced Materials* **2016**, *28*(14), 2777–2781, DOI: 10.1002/adma.201505491.

(4) Hirai, H.; Nakajima, K.; Nakatsuka, S.; Shiren, K.; Ni, J.; Nomura, S.; Ikuta, T.; Hatakeyama, T., One-Step Borylation of 1,3-Diaryloxybenzenes Towards Efficient Materials for Organic Light-Emitting Diodes, *Angewandte Chemie International Edition* **2015**, *54*(46), 13581–13585, DOI: 10.1002/anie.201506335.

(5) Lee, Y.-T.; Chan, C.-Y.; Tanaka, M.; Mamada, M.; Balijapalli, U.; Tsuchiya, Y.; Nakanotani, H.; Hatakeyama, T.; Adachi, C., Investigating HOMO Energy Levels of Terminal Emitters for Realizing High-Brightness and Stable TADF-Assisted Fluorescence Organic Light-Emitting Diodes, *Advanced Electronic Materials* **2021**, *7*(4), 2001090, DOI: 10.1002/aelm.202001090.

(6) Huang, Z.; Xie, H.; Miao, J.; Wei, Y.; Zou, Y.; Hua, T.; Cao, X.; Yang, C., Charge Transfer Excited State Promoted Multiple Resonance Delayed Fluorescence Emitter for High-Performance Narrowband Electroluminescence, *Journal of the American Chemical Society* **2023**, *145*(23), 12550–12560, DOI: 10.1021/jacs.3c01267.

(7) Wang, Y.; Duan, Y.; Guo, R.; Ye, S.; Di, K.; Zhang, W.; Zhuang, S.; Wang, L., A periphery cladding strategy to improve the performance of narrowband emitters, achieving deep-blue OLEDs with CIEy < 0.08 and external quantum efficiency approaching 20%, *Organic Electronics* **2021**, *97*, 106275, DOI: 10.1016/j.orgel.2021.106275.

(8) Jung, S.; Cheung, W.-L.; Li, S.-j.; Wang, M.; Li, W.; Wang, C.; Song, X.; Wei, G.; Song, Q.; Chen, S. S.; Cai, W.; Ng, M.; Tang, W. K.; Tang, M.-C., Enhancing operational stability of OLEDs based on subatomic modified thermally activated delayed fluorescence compounds, *Nature Communications* **2023**, *14*(1), 6481, DOI: 10.1038/s41467-023-42019-6.

(9) Jin, P.; Yang, X.; Su, W.-T.; Zhan, S.-H.; Chen, X.; Sun, H.; Yang, B.; Su, S.-J.; Hu, J.-Y., Narrow emission band ultraviolet/deep-blue thermally activated delayed fluorescence emitters modified with carbazole/carboline as a donor, *Journal of Materials Chemistry C* **2024**, *12*(48), 19498–19505, DOI: 10.1039/D4TC03503H.

(10) Xie, H.; Huang, Z.; Li, N.; Hua, T.; Miao, J.; Yang, C., Rational molecular design of TADF emitters towards highly efficient yellow electroluminescence with a nearly 30% external quantum efficiency and low roll-off, *Journal of Materials Chemistry C* **2022**, *10*(31), 11239–11245, DOI: 10.1039/D2TC02045A.

(11) Gao, Y.; Wang, Y.; Guo, Z.; Wan, Y.; Xue, Z.; Han, Y.; Yang, W.; Ma, X., Ultrafast photophysics of an orange–red thermally activated delayed fluorescence emitter: the role of external structural restraint, *Chemical Science* **2024**, *15*(17), 6410–6420, DOI: 10.1039/D4SC00460D.